

## NMR Spectroscopy and Atomic Force Microscopy Characterization of Hybrid Organic – Inorganic Coatings

Jiří Brus,\* Milena Špírková

Institute of Macromolecular Chemistry, Academy of Sciences of the Czech Republic,  
Heyrovského nám. 2, 162 06 Prague 6, Czech Republic  
E-mail: brus@imc.cas.cz

**Summary:** Hybrid organic–inorganic (O-I) epoxide-based products made from functionalized organosilicon precursors, oligomeric di- and triamines and in some cases colloidal silica particles were characterized by NMR spectroscopy and atomic force microscopy (AFM). The kinetics and reaction mechanism of condensation reactions, structure and segmental dynamics of final films, as well as homogeneity and partial ordering were studied by solid-state NMR spectroscopy (2D CRAMPS, 2D  $^1\text{H}$ - $^{13}\text{C}$  WISE, relaxation experiments); the surface morphology and other surface characteristics were determined by AFM.

**Keywords:** atomic force microscopy; coatings and films; solid-state NMR

### Introduction

New nanocomposite materials can be formed if controlled heterogeneity of the structure on the nanometer scale is possible. As the molecular-scale morphology plays an important role in achieving macroscopic properties of molecular and supramolecular assemblies, the synthetic goal is to prepare multiphase microheterogeneous systems with desired tunable properties. Organic–inorganic (O-I) hybrid polymers with an in situ created inorganic phase are considered as typical examples of such materials. The modification of organic matrix with silica–siloxane domains formed by the sol–gel process of alkoxysilanes is one of the methods of their preparation. The resulting structures depend on the reaction conditions used and vary from monodisperse silica particles to polymer networks.<sup>[1–6]</sup> Designing materials with well-adjusted properties makes possible their use in industrial applications with specific requirements, e.g., in the form of coatings as various kinds of protection<sup>[7–11]</sup>. [3-(Glycidyloxy)propyl]trimethoxysilane (GTMS) is one of the most used trialkoxysilane-type precursors.<sup>[12,13]</sup>

Recently, we have prepared and characterized a series of hybrid O-I coating films and free-standing films made from [3-(glycidyloxy)propyl]trimethoxysilane (GTMS), diethoxy[3-

(glycidyloxy)propyl]methylsilane (GMDES), poly(oxypropylene) of different molecular weights end-capped with primary amino groups (Jeffamine D-230, D-400 and T-403) and in some cases colloidal silica ( $\text{SiO}_2$ ) particles.<sup>[14,15]</sup> The variability of final properties was demonstrated on the base of static and dynamic mechanical analysis. It was found that it is possible to prepare products ranging from glassy through main transition up to rubbery state at room temperature. Although the composition and the techniques of preparation varied, all materials showing above-average values of toughness had temperature of glass transition close to 20 °C, that means they existed in the main transition region at room temperature.

This paper deals with the characterization of these O-I coating films. The structure development as well as homogeneity and partial ordering were studied by NMR spectroscopy while the surface morphology and other surface characteristics were determined by AFM.

## Experimental

**Materials:** [3-(Glycidyloxy)propyl]trimethoxysilane (GTMS, Fluka), diethoxy[3-(glycidyloxy)propyl]methylsilane (GMDES, Fluka), Jeffamine D230 and T403 (Huntsman Corporation, USA), colloidal silica (40 % solution in water;  $d = 29$  nm; Ludox AS-40, Aldrich) and propan-2-ol (Lachema, Czech Republic) were used as received. The formulas of Jeffamines are given in the Table 1.

**Technique of preparation of coating films:** GTMS and GMDES were mixed with water, propan-2-ol and (in some cases) with colloidal silica particles and stirred at ambient temperature for 24 h acid step. Then the proper amine was added and the reaction mixture was stirred at ambient temperature up to 3 h alkaline step and subsequently spread on glass or modified polypropylene sheets in a layer of constant thickness and immediately placed into an oven and kept at 80 °C (2h) and at 105 °C (1 h), (thermal curing).

**NMR spectroscopy:** The  $^1\text{H}$ ,  $^{13}\text{C}$  and  $^{29}\text{Si}$  MAS and CP/MAS NMR spectra were measured using a Bruker DSX 200 NMR spectrometer (Karlsruhe, Germany). The magic angle spinning (MAS) frequency was 4 kHz,  $B_1$  field intensity ( $^1\text{H}$  and  $^{29}\text{Si}$ ) corresponds to 62.5 kHz. The repetition delay was 10 s and the spin-lock pulse 2–5 ms. In the 1D and 2D  $^1\text{H}$  CRAMPS experiments, the BR-24 pulse sequence was used, with a 90° pulse length of 1.8  $\mu\text{s}$  and a large and short delay of 3.8 and 1.0  $\mu\text{s}$ , respectively. The MAS frequency was 2.5 kHz and the

repetition delay of 4 s.  $^1\text{H}$  scale was calibrated with an external standard – glycine (low field  $\text{NH}_3$  signal at 8.0 ppm and the high field  $\alpha\text{H}$  signal at 2.5 ppm). The spin diffusion mixing time was varied from 0.01 to 20 ms.

Table 1. The used Jeffamines

Abbreviation	Formula
D230	$\text{H}_2\text{N}-\underset{\text{CH}_3}{\text{CH}}-\text{CH}_2-\left(\text{O}-\underset{\text{CH}_3}{\text{CH}_2}-\text{CH}\right)_x-\text{NH}_2$ <p style="text-align: right;"><math>x = 2 - 3</math></p>
T403	$\begin{array}{c} \text{CH}_2-\left(\text{O}-\underset{\text{CH}_3}{\text{CH}_2}-\text{CH}\right)_x-\text{NH}_2 \\   \\ \text{CH}_3\text{CH}_2\text{C}-\text{CH}_2-\left(\text{O}-\underset{\text{CH}_3}{\text{CH}_2}-\text{CH}\right)_y-\text{NH}_2 \\   \\ \text{CH}_2-\left(\text{O}-\underset{\text{CH}_3}{\text{CH}_2}-\text{CH}\right)_z-\text{NH}_2 \end{array}$ <p style="text-align: right;"><math>(x + y + z) = 5 - 6</math></p>

**Atomic force microscopy (AFM):** Measurements were performed under ambient conditions using a commercial atomic force microscope (MultiMode Digital Instruments NanoScope™ Dimension IIIa). Olympus oxide-sharpened silicon nitride probes (OMCL TR-400, spring constants 0.02 and 0.08 N/m and OTR-8PS, spring constants 0.16 and 0.68 N/m) for the contact mode and an Olympus tapping-mode etched silicon probe (OTESPA, spring constant 42 N/m, resonant frequency 272 kHz) for the tapping mode were used. Moreover, a force modulation DT-FMR probe (Nanosensors, spring constant 2 N/m, frequency 70 kHz) was exercised as well.

## Results and Discussion

**NMR spectroscopy:** Several reaction mixtures were studied by NMR spectroscopy to follow the kinetics and reaction mechanism of polymerisation as well as to predict the final structures of resulting materials. During the acidic step, fast hydrolysis and formation of short oligomers

(dimers to tetramers) is the predominant process in systems without colloidal silica. Although the extensive polycondensation starts predominantly during the alkaline step the presence of colloidal silica in the reaction mixture accelerates condensation even at low pH. It seems that  $\text{NH}_4^+$  ions stabilizing colloidal silica particles promote the condensation reactions. Additionally it was found that no cleavage of oxirane rings occurs during the whole process before thermal curing, leaving these functional groups accessible to form organic network.

The structure of final coatings with the most suitable properties (prepared from GTMS, D230 and silica (GTMS/silica) and GMDDES, T403 and silica (GMDDES/silica)) was evaluated by analysis of  $^{13}\text{C}$  and  $^{29}\text{Si}$  CP/MAS NMR spectra as shown in Fig. 1a-d. Although it is generally accepted that the reactivity of alkylalkoxysilanes increases with increasing number of alkyl substituents, the condensation rate of GTMS ( $q=0.96$ ) is much higher than the condensation rate of GMDDES ( $q=0.77$ ) (see Fig. 1c and d).

This indicates formation of highly condensed and compact cage-like clusters, which are surrounded by organic phase. On the other hand, the presence of nearly 45%  $\text{D}^1$  units of the GMDDES monomer that are not fully condensed indicates formation of very short siloxane chains (on average tetramers – pentamers). The end  $\text{D}^1$  units do not increase the network density and thus provide only linkages between various chains. This fact results in significant softening of final coatings.

In  $^{13}\text{C}$  CP/MAS NMR spectra, the signals of the main structure

units were assigned (Fig. 1) using the standard editing technique CPPI<sup>18</sup>. Broadening of  $\text{CH}_2\text{-N}$

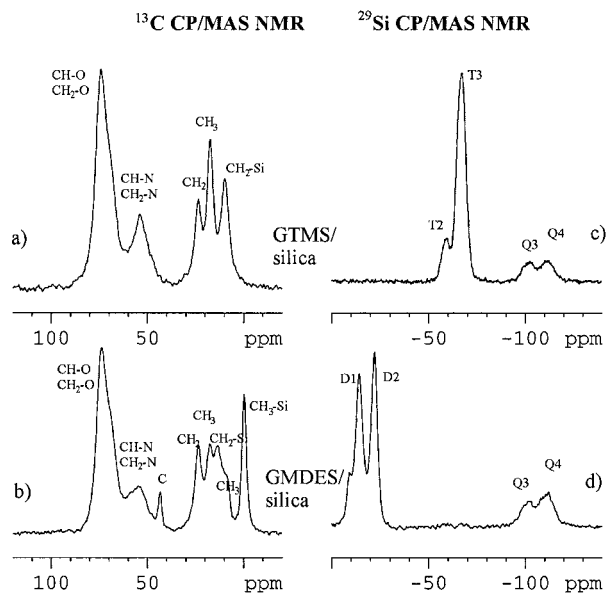


Figure 1.  $^{29}\text{Si}$  CP/MAS NMR and  $^{13}\text{C}$  CP/MAS NMR spectra: GTMS/silica system – (a) and (c), and GMDDES/silica system – (b) and (d), respectively.

and CH-N signals of the GMDDES/silica system indicates its worse conformational arrangement and disordering compared with the GTMS/silica one.

Relaxation measurements and 2D WISE NMR spectra reveal significant differences in segmental dynamics of the resulting materials. The estimated activation energies  $\Delta E$  of high-frequency motions (determined from variable-temperature  $T_1(^{13}\text{C})$  relaxation measurements) are remarkably lower for, e.g. CH-N, CH<sub>2</sub>-N (7 kJ.mol<sup>-1</sup>) and CH<sub>2</sub>-Si segments (5 kJ.mol<sup>-1</sup>) in the GMDDES/silica network, compared with the GTMS/silica one (41 and 22 kJ.mol<sup>-1</sup>; respectively). This corresponds to their large overall flexibility. In contrast, low-frequency motions (determined from variable-temperature  $T_{1\rho}(^{13}\text{C})$  relaxation measurements) of these CH-N, CH<sub>2</sub>-N (73 kJ.mol<sup>-1</sup>) segments are more hindered in the GMDDES/silica network compared with the GTMS system (47 kJ.mol<sup>-1</sup>) as a result of a smaller number of oxypropylene unit in amine moieties (Table 1). The exceptions are CH<sub>2</sub>-Si units in GMDDES/silica which when bonded to short siloxane chains, are not immobilized at all (29 kJ.mol<sup>-1</sup>). This confirms that these short siloxane chains lead to softening of final coatings and its larger elasticity. Low-frequency motions of CH<sub>2</sub>-Si groups in GTMS/silica networks are remarkably hindered (55 kJ.mol<sup>-1</sup>) as they are bonded to large compact cage-like clusters forming rigid siloxane-rich domains.

Variability in segmental dynamics in the GMDDES/silica system is quite clear from the 2D WISE NMR spectrum (Fig. 2), in which narrow and broad components for all signals are resolved. We found (from the spectrum measured with short CP, thus suppressing <sup>1</sup>H spin diffusion) that the narrow signal originates from Si-CH<sub>3</sub> units. Due to

spin-diffusion during the long cross-polarization step, magnetization is transferred to other <sup>1</sup>H species and thus its behavior is rapidly equilibrated. In our case, a high degree of equilibration (70-80 %) was achieved in 1 ms indicating intimate mixing of amine and siloxane residues and the absence of formation of larger heterogeneities in the organic phase of the GMDDES/silica system.

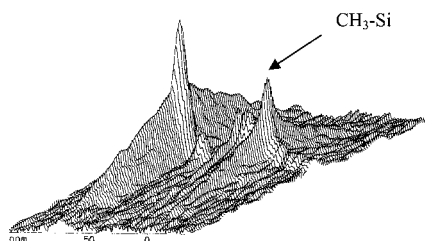


Figure 2. 2D <sup>1</sup>H-<sup>13</sup>C WISE NMR spectrum of the GMDDES/silica system.

2D  $^1\text{H}$  CRAMPS spin-diffusion experiments provide additional information about the ordering and arrangement of various components in complex systems. However, good spectral resolution is a necessary prerequisite. Unfortunately, this condition is not entirely fulfilled for our materials (see Fig. 3). We can resolve only three signals corresponding to  $\text{CH}_3\text{-Si}$  (-0.05 ppm),  $\text{CH}_3\text{-}$  and  $\text{CH}_2\text{-Si}$  (0.5 ppm), and other  $\text{CH}_2\text{-O}$  and  $\text{CH-O}$  (N) units (3.5 ppm). Due to this fact, we performed only qualitative analysis of 2D  $^1\text{H}\text{-}^1\text{H}$  CRAMPS spin-diffusion experiments (cf. Fig. 4). Off-diagonal signals in the 2D spectra correlating two different structure

units indicate their spatial proximity, and the dependence of off-diagonal signal intensity on spin-diffusion mixing time,  $t_m$ , corresponds to  $^1\text{H}\text{-}^1\text{H}$  interatomic distances and/or the size of domains in heterogeneous systems. In addition to all predictable signals a relatively weak diagonal signal (ca. 5.8 ppm) corresponding to hydrogen-bonded OH groups ( $\text{CH-OH}$  and/or  $\text{Si-OH}$ ) was found

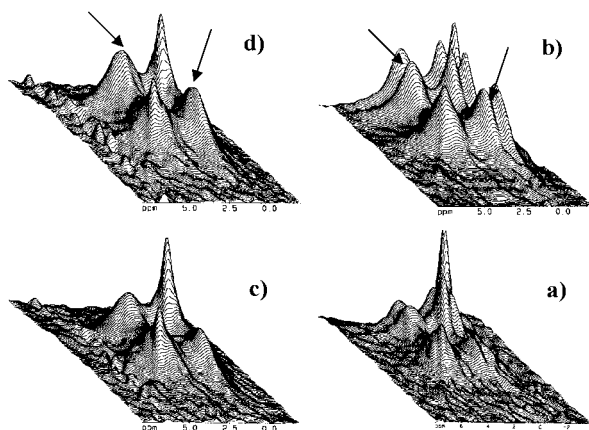


Figure 4. 2D  $^1\text{H}$  CRAMPS spectra of GMDES/silica (a) and (b) and GTMS/silica (c) and (d), measured with 250  $\mu\text{s}$  and 1 ms mixing time, respectively.

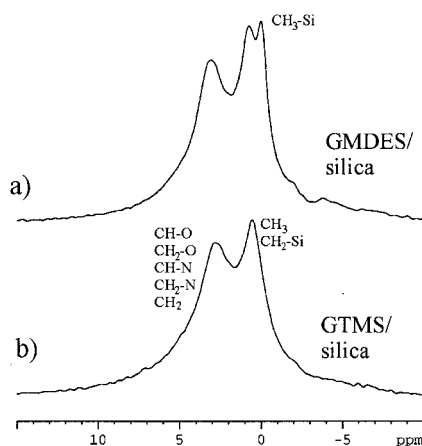


Figure 3.  $^1\text{H}$  CRAMPS spectra of the GMDES/silica (a) and GTMS/silica system (b).

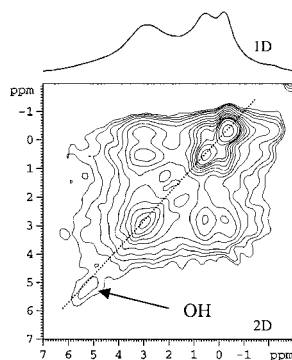


Figure 5. 2D  $^1\text{H}$  CRAMPS spectrum of GMDES/silica, measured with 250  $\mu\text{s}$  mixing time.

in 2D spectra of both materials (cf. Fig. 5). This indicates that also hydrogen-bonding interactions involving these OH groups can affect final mechanical properties of these films. Off-diagonal signals correlating at 3.5 and 0.5 ppm (in Fig. 4 marked by arrows) reflect mainly magnetization exchange between  $-\text{CH}_3$  and neighbouring  $-\text{CH}-\text{O}$  and  $-\text{CH}_2-\text{O}$  protons in one monomer unit. The rate of this magnetization exchange should be the same in similar networks, because this depends predominantly on the  $^1\text{H}-^1\text{H}$  interatomic distances. However, we observe significant differences (see Fig. 6). In GMDES/silica network,  $^1\text{H}$  magnetization is equilibrated after 0.5 ms, while in the GTMS/silica system after 0.85 ms. This indicates differences in ordering and arrangement of both components (originating from amine and siloxane monomers) in resulting networks, because a portion

of this cross-peak intensity reflects the long-range magnetization exchange between  $\text{CH}_2-\text{Si}$  protons and  $\text{CH}-\text{O}$  protons from the amine component. This means that there is longer average pathway through which  $^1\text{H}$  magnetization is transferred into GTMS/silica network. This can be explained by the formation of nano-heterogeneities in this network. The resulting material is formed by a

polycyclic cage-like siloxane phase, which is separated by the organic phase composed of oxypropylene units. Arrangement of organic chains is not random and we propose the formation of small domains formed by parallel or partially folded chains. This possibility follows from the application of D230, which is a linear molecule. On the other hand formation of such structures is less possible in the GMDES/silica system, due to the low condensation rate of siloxane structure units as well as due to the application of branched molecule of T 403. The resulting network is less organized and thus can be considered as almost homogeneous. The organic molecules of amine components are randomly linked by siloxane units. The structural characterization of final products studied by SAXS confirmed that GTMS/silica products differ substantially from GMDES/silica analogues. While GTMS/silica products exhibit a certain kind

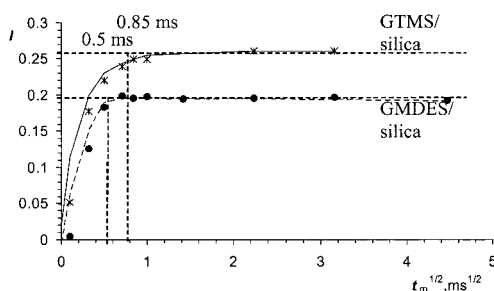


Figure 6. Dependences of cross-peak intensity (correlating 3.5 and 0.5 ppm) vs. mixing time: dots – GMDES/silica, asterisks – GTMS/silica.

of ordering (interference maximum), GMDES/silica products do not show any regular arrangement.<sup>[5]</sup>

**Atomic force microscopy:** The surface morphology and other surface characteristics were investigated by AFM in tapping and contact modes which were evaluated: (i) to test if any destruction of the surface may occur in the contact mode; (ii) to compare images of surfaces when either tapping or contact modes were applied.

(ia) Two images in the contact mode were performed: first scanning and then the tenth scan. If the condition of the minimum tip force on the sample surface was satisfied, identical images were obtained (even for samples with limited mechanical properties). No damage of surfaces by the probes occurs even for multiple scanning.

(ib) When normal forces of the probe on the sample were high enough (hundreds of  $\mu\text{N}$ ), it was possible to use the probe as a “scraper” and to determine microhardness and scratch resistance of coatings.<sup>[16,17]</sup> Figure 7 shows how non-destructive analysis (sample imaging, and 1) can be transformed into destructive conditions resulting in the formation of scrapes (2-4).

Figure 8 represents the top view characteristics of left-bottom detail of the image demonstrated in Fig. 7. Although the time (30 s) and the velocity and size of probe movement (4  $\mu\text{m/s}$ ; 350 nm) were kept the same in all cases, it is evident that the scrapes differ substantially in shape and depth depending on the value of the normal force applied. The destruction of surfaces in x-y coordinates (i.e., area damage) confirmed that hybrid O-I coating nanocomposite films are characterized by different local stiffness and elasticity on the nanometer scale.

(ii) The second main task was to decide what mode (tapping or contact) is more suitable for the surface characterization of hybrid O-I coatings. It is evident that equal information about surface morphology can be achieved for both modes, because the relief of the surface is preserved with slight differences not exceeding 1 nm in the maximum. Thus either tapping or contact mode can

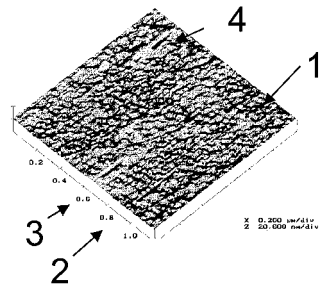


Figure 7. 3D image of the coating surface GTMS/silica system after destruction by OTR-8PS probe.

The normal force applied for 30 s onto the length 350 nm: 100nN (1); 170 nN (2); 240 nN (3); 370 nN (4).

Normal force used for imaging: 26 nN.



be used to achieve practically identical information about the surface morphology.

Based on the above-described measurements, the following can be concluded: All hybrid O-I coatings have fairly flat in nm units and regular surfaces; the surface smoothness and profile depend on the presence/absence of colloidal  $\text{SiO}_2$  particles. The presence of individual  $\text{SiO}_2$  nanoparticles at the surface is well apparent (Fig. 9). They are

distributed quite uniformly, without distinct clustering and they are well incorporated into the surface layer. It was calculated<sup>[15]</sup> that  $\text{SiO}_2$  nanoparticles, which are well miscible with all reactants and fairly compatible with the formed O-I networks, tend to concentrate in the surface

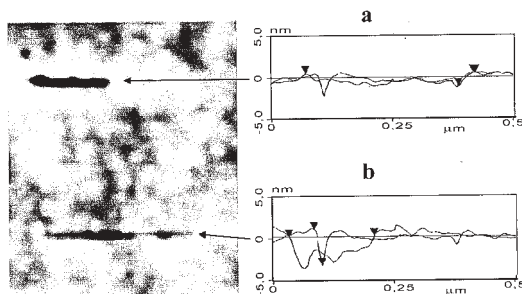


Figure 8. The shape of scratches after destruction of the coating surface by the probe.

Normal force: 170 nN (a); 240 nN (b). Length/depth<sub>max</sub> of the slot hole: 346 nm / 1.7 nm (a); 175 nm / 5 nm (b).

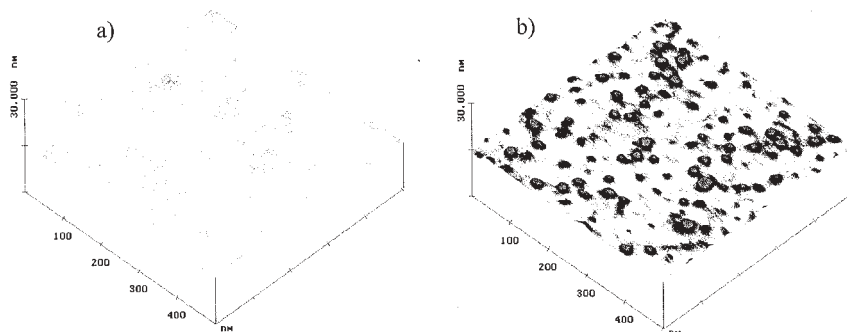


Figure 9. Examples of 3D images of sample surfaces: silica-free (a) and silica-containing (b) coatings; contact mode.

Composition of samples: GTMS, D230 (a); GMD, silica, T403 (b).

layer thus lowering the surface tension. However, a fraction of them still remains randomly distributed in the 3D structure as indicated by SAXS.<sup>[14]</sup>

## Conclusions

It was shown that advanced techniques of the solid-state NMR spectroscopy provide an important tool for investigation of the structure, arrangement and molecular dynamics at atomic and segmental level of complex organic-inorganic films. We found significant differences in the mechanism of formation of final structures, segmental dynamics and ordering as well as homogeneity of the prepared systems. While the systems composed of GMDES (bifunctional) and T403 (hexafunctional) monomers form a homogeneous, rather flexible random network without any ordering, which is incompletely condensed in the siloxane part, the system based on GTMS (trifunctional) and D230 (tetrafunctional) monomers forms nano-heterogeneous network with highly condensed cage-like siloxane clusters which are separated by the organic phase. The presence of these compact clusters leads to significant hindering of segmental motions. Surface morphology studied by AFM revealed that nanocomposite hybrid organic – inorganic coatings have very smooth and regular surface. If colloidal silica nanoparticles are present in the reaction system, they are very well detectable. Conditions for non-destructive analysis and controlled damage of surfaces (in order to study the scratch resistance) were evaluated.

## Acknowledgements

The authors wish to thank the Grant Agency of the Czech Republic (203/01/0735) and the Grant Agency of Academy of Sciences the Czech Republic (A 4050008) for financial support.

- [1] C. J. Brinker, C. W. Scherer, in: *'Sol-Gel Science'*, Academic Press, San Diego, 1990
- [2] E. J. A. Pope, J. D. Mackenzie, *J. Non-Cryst. Solids* **1986**, 87, 185.
- [3] J. C. Pouxviel, J. P. Boilot, J. C. Nelodil, J. Y. Lallemand, *J. Non-Cryst. Solids* **1987**, 89, 345.
- [4] N. S. M. Stevens M. E. Rezac, *Polymer* **1999**, 40, 4289.
- [5] Loy D A, B M Baugher, C R Baugher, D A Schneider and K Rahimian, *Chem. Mater.* **2000**, 12, 3624.
- [6] Fidalgo A , T G Nunes, and L M Ilharco, *J. Sol-Gel Sci. Technol.* **2000**, 19, 403.
- [7] J. Wen, V.J. Vasudevan, G. L. Wilkes, *J. Sol-Gel Sci. Technol.* **1995**, 5, 115.
- [8] T.L.Metroke, E.T.Knobbe, *Maert. Res. Proc. Res. Soc.* **2000**, Vol. 628, CC11.4.
- [9] R. Kasemann, H. Schmidt, *New J. Chem.* **1994**, 18, 1117.
- [10] F. Bauer, V. Sauerland, H.-J. Gläsel, H. Ernst, M. Findeisen, E. Hartmann, H. Langguth, B. Marquardt, R. Mehnert, *Macromol. Mater. Eng.* **2002**, 287, 546.
- [11] H. Ni, A. H. Johnoson, M. D. Soucek, J. T. Grant, A. J. Vreugdenhil, *Macromol. Mater. Eng.*, **2002**, 287, 470.
- [12] M.W. Daniels, L.F. Francis, *J. Colloid Interface Sci* **1998**, 205, 191.
- [13] L. Matějka, O. Dukh, J. Brus, W. J. Simonsick, B. Meissner, *J. Non-Cryst. Solids* **2000**, 270, 34.
- [14] M. Špírková, J. Brus, D. Hlavatá, H. Kamišová, L. Matějka, A. Strachota, *J. Appl. Polym. Sci.*, submitted
- [15] M. Špírková, J. Brus, D. Hlavatá, H. Kamišová, L. Matějka, A. Strachota, *Surf. Coat. Int.*, submitted
- [16] W. Shen, S.M. Smith, F.N. Jones, C. Ji, R.A. Ryntz , M.P. Everson, *J. Coat. Technol.* **1997**, 69, 123.
- [17] M. W. Bai, K. Kato, N. Umehara, Y. Miyake, J.G. Xu, H. Tokisue, *Surf. Coat. Technol.* **2000**, 126, 181.
- [18] X. Wu, S.T. Burns, K.W. Zilm, *J. Magn. Reson A* **1994**, 111, 29.